JOURNAL OF VIROLOGY, July 1994, p. 4514–4524
0022-538X/94/$04.00+0

Vol. 68, No. 7

Mutations in Accessory DNA Replicating Functions Alter the Relative Mutation Frequency of Herpes Simplex Virus Type 1 Strains in Cultured Murine Cells

RICHARD B. PYLES AND RICHARD L. THOMPSON*

Department of Molecular Genetics, Biochemistry and Microbiology, College of Medicine, University of Cincinnati, Cincinnati, Ohio 45267-0524

Received 16 December 1993/Accepted 11 April 1994

The contribution of the herpes simplex virus type 1 (HSV-1)-encoded uracil DNA glycosylase (UNG), thymidine kinase (TK), and dUTPase to the relative mutant frequency (RMF) of the virus in cultured murine cells was examined. A panel of HSV-1 mutants that lacked singly or doubly the UNG, TK, or dUTPase activity were generated by disruption of the enzyme coding regions with the *Escherichia coli* β-galactosidase (β-gal) gene in strain 17syn$^+$. To establish a baseline RMF of strain 17syn$^+$, the β-gal gene was inserted into the UL3 locus. In all of the viruses, the β-gal insert served as a phenotypic marker of RMF. A mutant plaque was identified by the lack of β-gal activity and, in selected cases, positive in situ hybridization for β-gal sequences. Replication kinetics in NIH 3T3 cells demonstrated that all of the mutants replicated efficiently, generating stocks with equivalent titers. Two independently generated UL3–β-gal viruses were examined and established a baseline RMF of ~0.5% in both NIH 3T3 and LM TK$^-$ cells. Loss of dUTPase activity resulted in viruses with fivefold-increased RMFs, indicating that the HSV-1 dUTPase has an antimutator function. The RMF observed for the tk$^-$ viruses was reduced as much as 40-fold (RMF of 0.02%), suggesting that the viral TK is a mutator activity. The RMF of two independent UNG$^-$ viruses showed no significant difference from the baseline RMF in limited passage; however, following successive passage, the data suggested that UNG activity serves as an antimutator. These results have implications for the natural history of HSV and the development of antiviral therapies.

Herpes simplex virus (HSV) is one of the most complex animal viruses, encoding over 70 genes within its 152-kb double-stranded DNA genome (35). Included among these are a number of enzymatic activities which are involved in the replication of the viral genome (4, 35). As has been shown in other DNA viruses, such as bacteriophage T4 (2, 10, 28, 44), HSV type 1 (HSV-1) has evolved mutation strategies that presumably provide a selective advantage to the virus. In a series of reports, Hall and colleagues have demonstrated that the HSV-1 DNA polymerase (DNA pol; 18–20), like the T4 DNA pol, has a low fidelity of deoxynucleoside triphosphate selection that serves as a mutator function (20). Such polymerase activities would result in a relative mutant frequency (RMF) dependent upon the nucleotide pool sizes present during viral DNA replication. Therefore, the virally encoded enzymes that modulate nucleotide pool size and replication fidelity may also play a significant role in viral RMFs. An understanding of the viral factors contributing to the RMF of the virus and thus influencing the rate of development of drug-resistant progeny is crucial to effective antiviral therapy.

Regulation of mutation frequencies is of obvious importance to the success of the virus. For example, naturally occurring drug-resistant progeny are rapidly selected in culture (32, 40, 41) and following antiviral therapy in patients (3, 12, 38, 42). RMFs that are too low or artificially inhibited may limit the viruses' ability to escape a host's immune response or antiviral therapies. Conversely, viral RMFs that are too high would lead to an unacceptable level of nonviable progeny. Antiviral therapies that include perturbation of viral controls of RMF could improve the efficiency of treatment of viral disease.

HSV provides an excellent model system to gain an understanding of the virally encoded functions which contribute to the RMF, as the virus replicates well in a large variety of cellular environments (17); viral mutants are easily generated, and a great deal of work has already been completed on the virally encoded enzymes that promote efficient DNA replication.

In this report, a system to establish the viral RMF of a nonselected transgene, that for β-galactosidase (β-gal), in the context of viral strains which lack enzyme activities associated with viral DNA replication is described. β-Gal activity converts the chromagen X-Gal (5-bromo-4-chloro-3-indolyl-β-D-galactopyranoside) into a blue precipitate and therefore serves as a phenotypic marker for individual plaques. Loss of β-gal activity due to mutation results in a clear (nonblue) plaque which has been genotypically confirmed by in situ hybridization. Specifically, the relative contribution of the HSV-1-encoded thymidine kinase (TK), dUTPase, and uracil DNA glycosylase (UNG) activities to the viral RMF following propagation in NIH 3T3 and LM TK$^-$ cell lines was established. The baseline RMF of strain 17syn$^+$ was determined by analysis of mutants in which the β-gal gene was inserted into the UL3 locus. Analysis of the passage stocks of these mutants established an averaged baseline RMF of ~0.5% or one mutant in every 200 PFU. In comparison, the RMFs established for the other mutants demonstrated that the HSV-1-encoded TK provides a potent mutator activity, the viral dUTPase has an antimutator function, and viral UNG activity has no appreciable effect on RMFs in limited passage but may be an antimutator following successive rounds of replication. The implications of these data

* Corresponding author. Mailing address: Dept. of Molecular Genetics, Biochemistry and Microbiology, University of Cincinnati Medical Center, P.O. Box 670524, Cincinnati, OH 45267-0524. Phone: (513) 558-0062. Fax: (513) 558-8474.

are discussed with respect to HSV replication and antiviral therapies.

MATERIALS AND METHODS

Cell lines and viruses. Rabbit skin cells (RSC) were cultured as previously described (46). RSC monolayers were used to generate the recombinant viruses, as well as viral stocks and viral genomic DNA, as previously described (46). NIH 3T3 (ATCC CRL 6442) cells are a homogeneous murine fibroblast cell line and were used for passage of the virus panel to examine RMF. NIH 3T3 monolayers were cultured in Dulbecco's modified Eagle medium (GIBCO/Bethesda Research Laboratories, Gaithersburg, Md.) supplemented with 10% fetal bovine serum at 37°C–5% CO_2 in a humidified atmosphere. A second murine cell line, LM TK^-, was used for a single passage of a subset of the virus panel. LM TK^- (ATCC CCL 1.3) cells were cultured as described for NIH 3T3 cells.

Virus strains used in this study were derived from wild-type (wt) HSV-1 strain $17syn^+$, which was obtained from J. Subak-Sharpe of the Medical Research Council Virology Unit in Glasgow, Scotland. The derivation and history of $17syn^+$ have been previously described (46). Base pair numbering, restriction endonuclease maps, and restriction fragment names are based upon the complete sequence of HSV-1 strain $17syn^+$ compiled by McGeoch and colleagues (29). The methods used for viral titrations, as well as determination of in vitro replication kinetics, have been described (46).

Production of recombinant viruses. The panel of recombinant viruses analyzed in this study, with the exceptions of tBd and 1602A, were generated by cotransfection of unit length $17syn^+$ genomic DNA and modified, cloned $17syn^+$ DNA fragments. tBd and 1602A are double mutants derived from $17syn^+$-based, dUTPase-negative strain dUT^-1218, which was provided by V. Preston (14). The viruses were designed to assess the contribution of each of the specified HSV-1 enzyme activities to the RMF of the virus. Insertional mutations were chosen to minimize genomic perturbations and to provide a readily assayed marker for RMF.

To construct the mutations, fragments of $17syn^+$ genomic DNA containing the open reading frames (ORF) of interest were cloned into pUC19 by standard methods. Mutation of the selected genes was accomplished by insertion of a 4-kb *Xba*I simian virus 40 early promoter–β-gal cassette isolated from plasmid pFJ3 (a kind gift of D. McGeoch [30]). The β-gal cassette was inserted into the genes of interest at sites that disrupted the ORF but left the neighboring ORF unaffected. Upon incorporation into the viral genome, the β-gal insert served as a reporter of recombination and allowed simplified selection of recombinants.

Cotransfections were performed with LipofectACE (GIBCO/Bethesda Research Laboratories) in subconfluent RSC monolayers. Briefly, an empirically optimized amount of genomic viral DNA and the specific mutated fragment were incubated for 15 min with 10 μl of LipofectACE in serum-free culture medium (minimal essential medium) at room temperature (total volume, 1 ml). This mixture was applied to RSC monolayers which were incubated for 4 h and then fed with normal growth medium (minimal essential medium supplemented with 5% newborn calf serum). The medium was exchanged with fresh growth medium after approximately 12 h. Plaques developed 36 to 48 h posttransfection and were then overlaid with agarose containing the chromagenic substrate X-Gal (Fisher) at 125 μg/ml. Plaques formed by recombinant viruses converted the X-Gal into a blue precipitate. Blue plaques were isolated and plaque purified to homogeneity. The genomic structure of each of the viruses is depicted schematically in Fig. 1. Specifics of the viral mutations are described below.

Two independent control viruses, 3B1 and 3B2 ($UL3^-$ blue isolates 1 and 2), were generated from separate cotransfection cultures. These two viruses carry the Klenow-filled *Xba*I β-gal cassette inserted at the *Eco*RV site (bp 11084) within the UL3 ORF (bp 10959 to 11664). The mutation was generated within the cloned $17syn^+$ *Bam*HI e fragment (bp 2907 to 11820).

uB1 and uB2 (UNG^- blue isolates 1 and 2) are two virus isolates from independent cotransfections carrying the *Xba*I β-gal cassette at the *Xba*I site (bp 10636) within the UNG ORF (UL2, bp 9886 to 10888). This mutation was also generated in the cloned *Bam*HI e fragment.

Mutation of the $17syn^+$ TK was accomplished by insertion of the filled *Xba*I β-gal cassette at the *Sna*BI site (bp 47560) within the TK-encoding gene (UL23; bp 47802 to 46674) contained within the cloned $17syn^+$ *Bam*HI p fragment (bp 45055 to 48634). Recombination of the TK^-–β-gal fragment into $17syn^+$ resulted in the isolation of tB (TK^- blue).

The gene for dUTPase (UL50, bp 107010 to 108123) also was mutated by insertion of the filled *Xba*I β-gal gene at the *Asp*718 site (bp 107305) which had been blunt ended with Klenow (GIBCO/Bethesda Research Laboratories). Following cotransfection of the dUTPase–β-gal construct and $17syn^+$, viral strain dB (dUTPase$^-$ blue) was isolated. Previous work with engineered HSV-1 mutant strain dUT^- 1218, generated by Fisher and Preston, demonstrated that insertion of a 12-bp *Hin*dIII linker at the *Asp*718 site at bp 107305 in $17syn^+$ eliminated HSV-1-induced dUTPase activity (14).

The two virus isolates that carry double mutations were derived from dUTPase-negative HSV-1 mutant strain dUT^-1218. The first double mutant, tBd, was generated by recombination of the TK^-–β-gal construct with unit length dUT^-1218 genomic DNA. This virus lacks both HSV-1-induced TK and dUTPase activities. Virus isolate 1602A was plaque purified from a stock of virus kindly provided by D. McGeoch (30). McGeoch and colleagues generated the original 1602 stock by cotransfection of a UNG^-–β-gal construct with dUT^-1218 genomic DNA, resulting in a UNG^-, dUTPase-negative derivative of strain $17syn^+$. The orientation of the β-gal insert in 1602A is opposite to that of uB1 and uB2.

Southern blot-restriction fragment length polymorphism analysis was performed as previously described (43) and confirmed the genomic structures and stock purity of all of the viruses used in this study. Restriction enzymes were purchased from GIBCO/Bethesda Research Laboratories. Digestions were performed under the conditions recommended by the manufacturer.

RMF assay. For RMF analyses, virus passage stocks were generated in either NIH 3T3 or LM TK^- monolayers. Passage 1 (P1), P1′, and LM TK^- P1 stocks were produced by low-multiplicity-of-infection (MOI) (0.01 PFU per cell) infection of NIH 3T3 (P1 and P1′) or LM TK^- (LM TK^- P1) cells. The NIH 3T3 P1 stock is also the 96-h time point presented in the replication kinetic experiments. Passage 2 (P2) represents viral stocks generated by low-MOI (0.01 PFU per cell) infection of NIH 3T3 monolayers with the P1 stocks. HP designates viral stocks produced by high-MOI (3 to 5 PFU per cell) infection of NIH 3T3 cells with the original viral stocks.

For each of the passages, triplicate cultures were generated, pooled, and subjected to three cycles of freezing and thawing. Aliquots (~2,000 PFU) of each passage were adsorbed onto 100-mm-diameter RSC monolayers for 1 h and then overlaid with culture medium supplemented with 0.03% human immune globulin (165-mg/ml stock; Gammar). The plates were

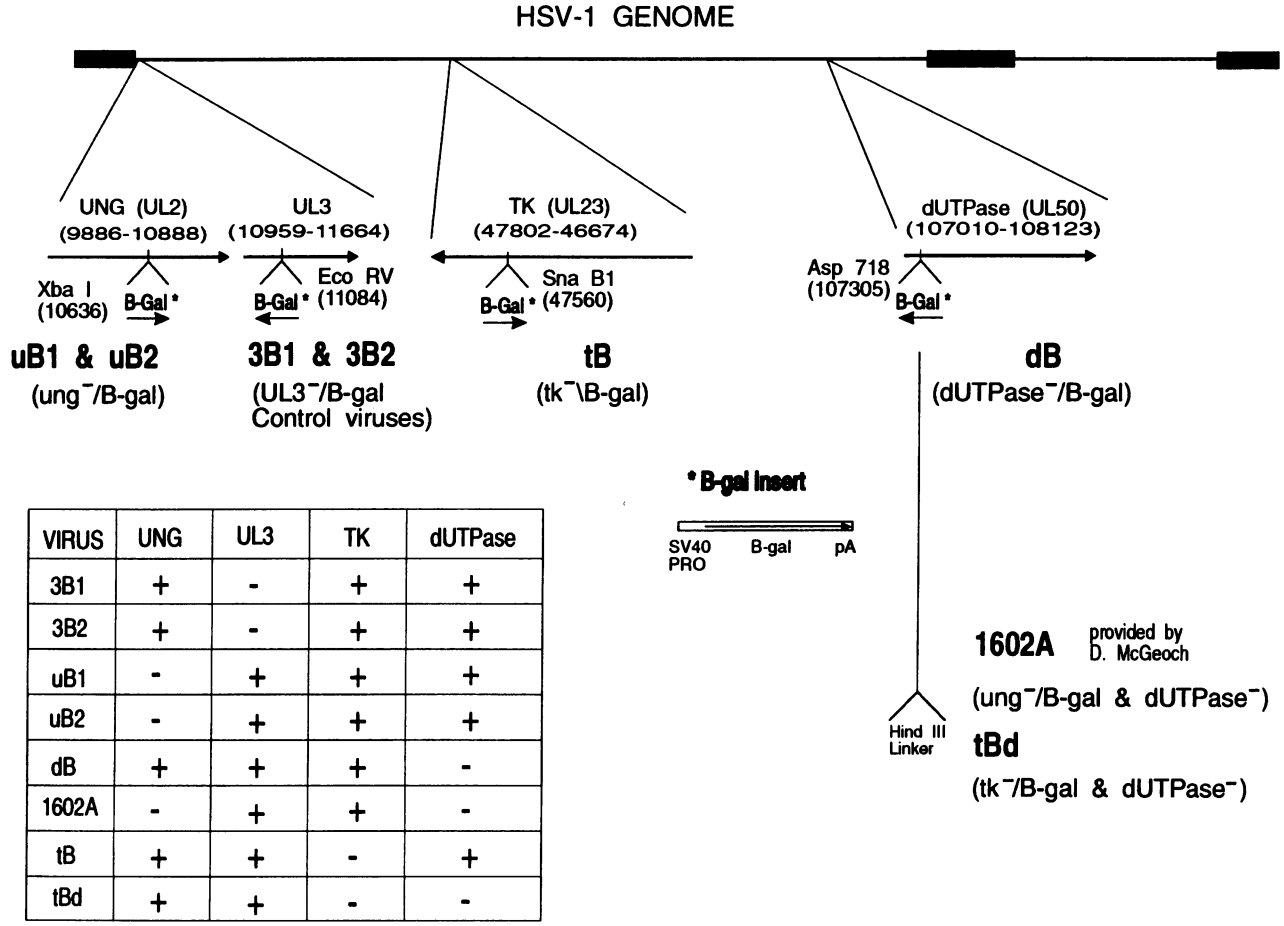

VIRUS	UNG	UL3	TK	dUTPase
3B1	+	-	+	+
3B2	+	-	+	+
uB1	-	+	+	+
uB2	-	+	+	+
dB	+	+	+	-
1602A	-	+	+	-
tB	+	+	-	+
tBd	+	+	-	-

FIG. 1. Schematic of the mutations in the viral panel. The top line is a schematic representation of the 152-kb HSV-1 genome. The thick segments are representative of the terminal and internal repeat elements of the HSV-1 genome. The arrows below the genome depict the transcripts of interest and the approximate locations of the indicated ORF. Restriction enzyme sites of interest are indicated. The site of disruption by insertion of the β-gal cassette is indicated. The β-gal cassette contains the *E. coli* β-gal gene under control of the simian virus 40 early promoter (SV40 PRO) and is terminated by the simian virus 40 poly(A) signal (pA) and is also depicted. The table shows the enzyme activities encoded by each of the engineered viruses. Note that control viruses 3B1 and 3B2 are independent isolates and carry functional UNG, TK, and dUTPase enzymes.

maintained for ~48 h, until obvious plaques appeared, and were then fixed for 5 min with a solution of 2% paraformaldehyde–0.2% glutaraldehyde–0.01% Nonidet P-40 at 4°C. The fixed monolayers were rinsed with phosphate-buffered saline (PBS) and then incubated with X-Gal in buffer [X-Gal at 125 μg/ml in 5 mM $K_3Fe(Cn)_6$–5 mM $K_4Fe(Cn)_6$–2 mM $MgCl_2$–0.01% Nonidet P-40]. Following overnight incubation at 37°C, the monolayers were rinsed with PBS and counterstained red with Ponceau S to visualize clear plaques more easily. The plates were observed at a magnification of ×40 with a Nikon TMS microscope. Photomicrographs of selected plates were generated with TMAX-100 film (Kodak) with an image magnification of ~×20.

The plaques on each plate were counted by using a grid background (4 mm square; ~1 microscope field) to map any clear plaques observed. In cases of excessive cytopathic effect, entire grid squares were eliminated from the counts. Chi-square analysis with the Yates continuity factor was performed on the compiled data. Populations of 2,587 plaques were determined in advance to be sufficient to prevent type I or II errors with 95% confidence.

In situ hybridization. The in situ hybridization procedure used to detect the β-gal-specific sequences in viral plaques was adapted from the procedure of Smith (39). A β-gal-specific probe was generated by random priming with dUTP labeled with digoxigenin (DIG) by using the manufacturer's protocol (Genius kit; Boehringer Mannheim). Selected X-Gal-stained plates were rinsed with phosphate-buffered saline to remove the Ponceau S counterstain and then incubated with 125 μg of pronase (Boehringer Mannheim) per ml in SSPE (90 mM NaCl, 10 mM NaH_2PO_4, 10 mM EDTA, pH 7.4) for 30 min at 37°C. The plates then were rinsed with SSPE and treated with 0.2 N HCl for 10 min at room temperature. Following 5 min of postfixation in 4% paraformaldehyde, the plates were rinsed extensively with SSPE and then prehybridized for at least 2 h at 42°C in a solution of 50% formamide (Fisher)–SSPE–0.1% sodium dodecyl sulfate–5× Denhardt's solution (1× Denhardt's solution is 0.2% Ficoll [type 400; Sigma], 0.2% polyvinylpyrrolidone, and 0.2% bovine serum albumin [fraction V; Sigma]–20 μg of denatured herring sperm DNA (Sigma) per ml. Hybridization of the DIG-labeled β-gal probe (added at ~500 ng/ml) proceeded overnight (16 h) at 42°C. The plates

were washed in 2× SSC (1× SSC is 0.15 M NaCl and 0.015 M sodium citrate) at 42°C with several changes of buffer, followed by several room temperature washes in 0.1× SSC.

Immunohistochemical detection of the hybridized probe was performed by using anti-DIG Fab fragment conjugated to alkaline phosphatase (Boehringer Mannheim). The plates were preincubated in a 1% blocking solution (1% [wt/vol] Genius kit blocking reagent in 100 mM Tris–150 mM NaCl, pH 7.5 [Genius buffer 1]) for 30 min at room temperature. The anti-DIG Fab fragment was added at a 1:250 dilution in the 1% blocking solution and incubated for 1 to 2 h. Following several washes with Genius buffer 1, the plates were treated with a prepared solution of Histomark Red (Kirkegaard & Perry). Following incubation for 1 h to overnight, a red precipitate formed in the presence of the alkaline phosphatase conjugate. By using the previously generated grid map to locate the clear (nonblue) plaques, the plates were reexamined and scored for the presence of the β-gal gene.

RESULTS

Recombinant virus panel. The genomic structures of the recombinant viruses are shown schematically in Fig. 1. Insertion of the ~4-kb β-gal cassette served three functions in the study. First, the β-gal gene was used to disrupt the enzyme ORF without affecting the neighboring ORFs. Second, upon incorporation into the 17syn$^+$ genome, β-gal activity served as a phenotypic marker of recombination, expediting virus purification. Third, the β-gal gene served as a "phenotypic sink" for mutations acquired during replication of the virus.

Following plaque purification of the recombinant viruses, viral DNA was prepared and analyzed by Southern blot-restriction fragment length polymorphism analysis as previously described (43). A representative Southern blot of *Asp*718-digested viral DNAs was hybridized successively to the indicated ^{32}P-labeled probes and is shown in Fig. 2. By this assay, all of the viral stocks were found to be pure, with no contaminating wild-type bands evident following hybridization with the mutation locus-specific probe.

Following hybridization with the radiolabeled 4-kb β-gal probe, all of the mutant viruses demonstrated the expected fragment(s). No hybridization was detected in the 17syn$^+$ lane. Addition of the *Asp*718 site and the 4-kb β-gal sequence at the UL3 locus (Fig. 1) resulted in two novel bands of 5,732 and 10,994 bp evident following hybridization with either the β-gal or UNG-UL3 probe (lanes 3B1 and 3B2). The wild-type *Asp*718 fragment, which contains the UL3 and UNG (UL2) genes, is 12,610 bp long and is evident on the UNG-UL3 blot (for example, the 17syn$^+$ lane). The smaller bands evident in the tB, dB, and tBd viral samples (which have unaltered UNG-UL3 regions) are due to hybridization of the viral β-gal sequences to the pUC19 vector included in the UNG-UL3 probe.

Hybridization of *Asp*718-digested uB1 and uB2 DNAs with the β-gal or UNG-UL3 probe resulted in two fragments of 7,524 and 9,202 bp (lanes uB1 and uB2 on the β-gal and UNG-UL3 blots). These novel fragments again resulted from insertion of the *Asp*718 site and the 4-kb β-gal sequence. Most of the β-gal cassette is contained in the 9,202-bp fragment, as shown following hybridization to the β-gal probe. Following hybridization to the UNG-UL3 probe, which should bind primarily to the 7,524-bp fragment, the intensities of hybridization are reversed. Mullaney et al. demonstrated that a 17syn$^+$-derived virus, designated *in*1601, which carried the same UL2 locus mutation, was UNG$^-$ but fully replication competent and concluded that the HSV-1 UNG is dispensable for replication in cultured cells (30). The β-gal insertion at the UNG locus in double mutant 1602A is in the opposite orientation to the insertion in uB1 and uB2. Following *Asp*718 digestion of 1602A viral DNA, two novel fragments of 6,200 and 10,526 bp were evident (β-gal and UNG-UL3 blots).

Insertion of the β-gal cassette into the TK ORF resulted in two novel fragments of 3,599 and 5,493 bp following *Asp*718 digestion of tB and tBd viral DNAs (TK blot). The expected *Asp*718 wild-type 4,959-bp fragment was evident in all of the other viruses following hybridization to the TK-specific probe (bp 47053 to 47893). Three independent measures of TK activity, including arabinosylthymine resistance, phosphorylation of [^{3}H]thymidine, and [^{14}C]thymidine plaque autoradiography, demonstrated that the mutation in tB eliminated HSV-1-induced TK activity (31a).

Owing to the cloning procedure used to disrupt the dUTPase gene, the *Asp*718 site of insertion (bp 107305) was regenerated at each end of the β-gal insert, resulting in the presence of the 3,549-bp, promoterless β-gal gene (Fig. 2, β-gal blot, lane dB). Mutation at this site has previously been shown to eliminate HSV-1 dUTPase activity (14, 50). Hybridization of the dUTPase-specific probe (bp 105105 to 110095) demonstrated the two expected wild-type bands (*Asp*718 fragments u and o, 2,772 and 4,680 bp, respectively) in all of the viruses except the two double mutants. These bands were expected in dB, as the insertion is released by digestion with *Asp*718. In addition to these two fragments, the fragments containing the β-gal sequence are visible in the recombinant virus lanes also, because of the presence of vector sequences in the dUTPase probe.

Double mutants tBd and 1602A were derived from HSV-1 strain 17syn$^+$ dUTPase-negative mutant dUT$^-$1218 (14), in which the *Asp*718 site at bp 107305 was converted to a *Hin*dIII site (Fig. 1). This mutation resulted in fusion of the *Asp*718 u and o fragments, producing a novel fragment of 7,464 bp (lanes tBd and 1602A). Probing of this blot and others with additional regions of the HSV-1 genome demonstrated no unexpected genomic perturbations (data not shown).

Replication kinetics of the viruses in NIH 3T3 cells. To assess the RMF of the HSV-1 strains, it was necessary to establish that the mutant viruses replicated equivalently in cultured cells. Single-step replication kinetic analyses with NIH 3T3 monolayers confirmed that no general replication defect was present in any of the viruses (Fig. 3, top panels). Since the effect of any replication defect would be expected to become more pronounced with successive rounds of replication, multistep kinetics were compiled following low-MOI (0.01 PFU per cell) infection of NIH 3T3 monolayers. The results of these assays demonstrated no difference in the replication abilities of the viruses. In all cases, the mutant viruses attained peak titers roughly equivalent to those of 3B1 and 3B2 (Fig. 3, lower panels), and in other experiments they attained peak titers equivalent to those of strain 17syn$^+$ (data not shown).

Together, these data confirmed that each of the enzymes and the UL3 gene product are dispensable for viral replication in NIH 3T3 cells, in agreement with results reported previously for many other cell lines (1, 14, 23, 30). In addition, no selective advantage or disadvantage was detected in the viruses containing the β-gal insert, allowing accurate estimation of the viral RMF on the basis of phenotypic loss of β-gal activity.

RMF assay. Previous examinations of the frequency of viral mutants in stocks of wild-type HSV-1 strains have demonstrated a range of RMFs varying from 0.001 to >1% (18–20, 31, 40, 41). In these studies, mutant plaques were identified by resistance to anti-HSV compounds in the culture media used.

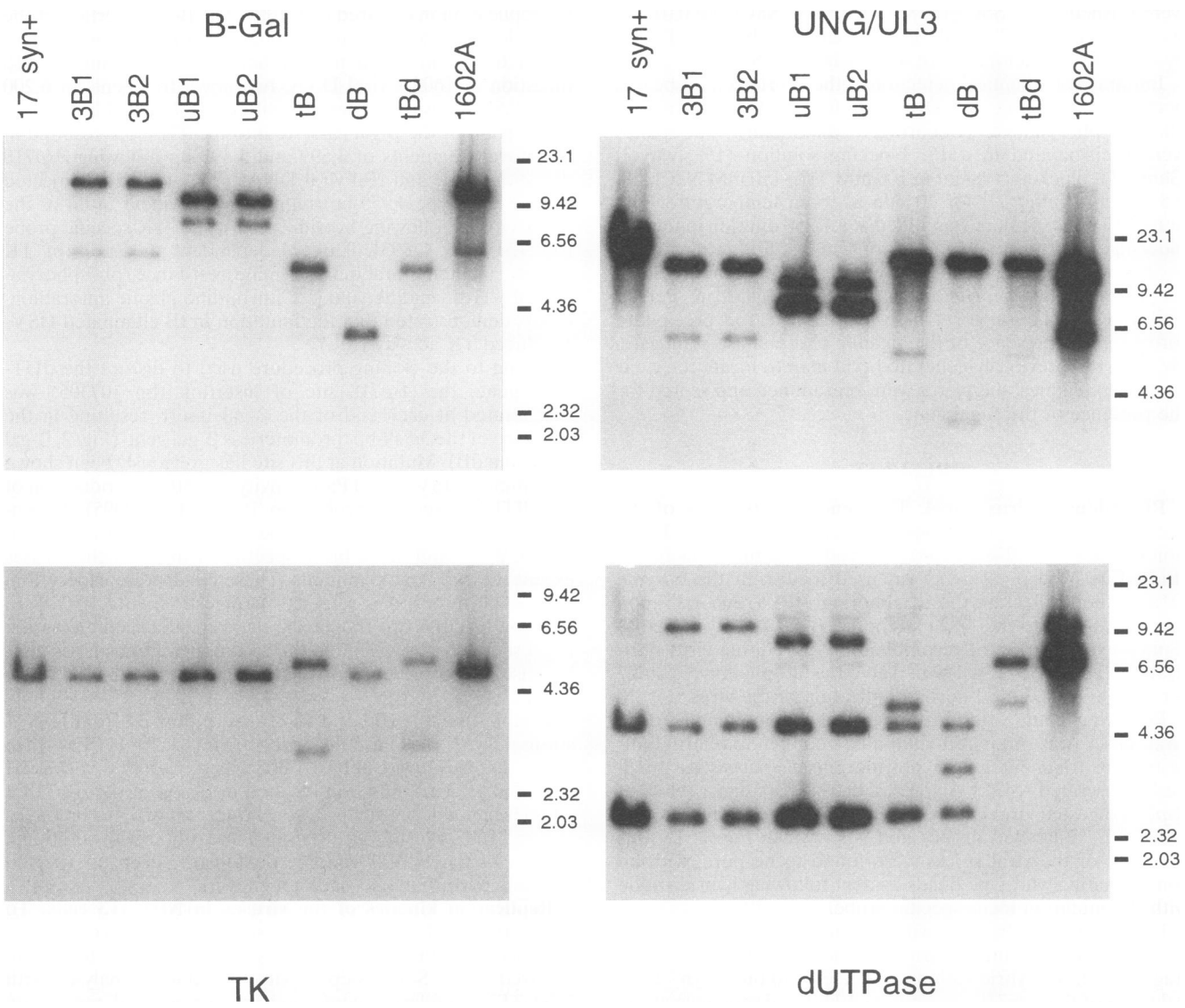

FIG. 2. Southern blot-restriction fragment length polymorphism analysis of the viruses employed in this study. Following digestion with restriction enzyme *Asp*718, the viral DNA fragments were separated in 0.8% agarose and transferred to nitrocellulose as previously described (43). The indicated ^{32}P-labeled probes described in the text were hybridized successively to the blot to demonstrate the genomic structures of the viruses. The sample source is indicated above the blot. Migration of the DNA size markers (in kilobase pairs) is denoted on the side of each blot.

In other studies, drug resistance was mapped to the viral TK and DNA *pol* genes (5, 36), suggesting two possible types of mutations quantitated by this method. Hall and colleagues were the first to map a mutator function to a specific HSV-1-encoded protein, demonstrating that antimutator strains of HSV-1 encode a modified DNA *pol* with increased fidelity of deoxynucleoside triphosphate selection (20). In these studies, stocks of HSV-1 were generated following infection of cultured cells at an MOI of 0.01 PFU per cell and then plated in the presence of antiviral compounds directed to the viral TK activity. Mutants were quantitated by the number of plaques that formed in the presence of the antiviral compound. This system is not suitable for assessment of the contribution of the viral TK to RMFs. In addition, TK mutations may also be a disadvantage to the virus (13, 22, 45) and therefore be selected against. Accurate estimation of the RMF is complicated by the fact that the nonmutant plaques did not form, allowing only an estimation of the total population assayed.

To establish the RMF of HSV-1 strain 17syn$^+$ derivatives in cultured murine cells, a system was developed that employs a nonselected phenotypic marker (β-gal). Stocks of virus strains carrying this marker were prepared as described in Materials and Methods following infection (0.01 PFU per cell) of NIH 3T3 monolayers. Aliquots of ~2,000 PFU of the passage stocks were assayed on RSC monolayers for the β-gal phenotype of individual PFU by histochemical staining with X-Gal. A mutant was identified as a clear plaque (Fig. 4, top panels).

To confirm that clear plaques observed in the passage stocks were true mutants (β-gal activity negative) and did not represent contamination with the parental wild-type virus (β-gal gene negative), in situ hybridization was performed on selected plates. Control 17syn$^+$ plaques did not cross-react with the probe, indicating that the in situ hybridizations were specific for β-gal sequences (data not shown). As can be seen in the bottom panels of Fig. 4, mutant plaques are identified by lack of the blue X-Gal precipitate (darkly stained cells at the plaque

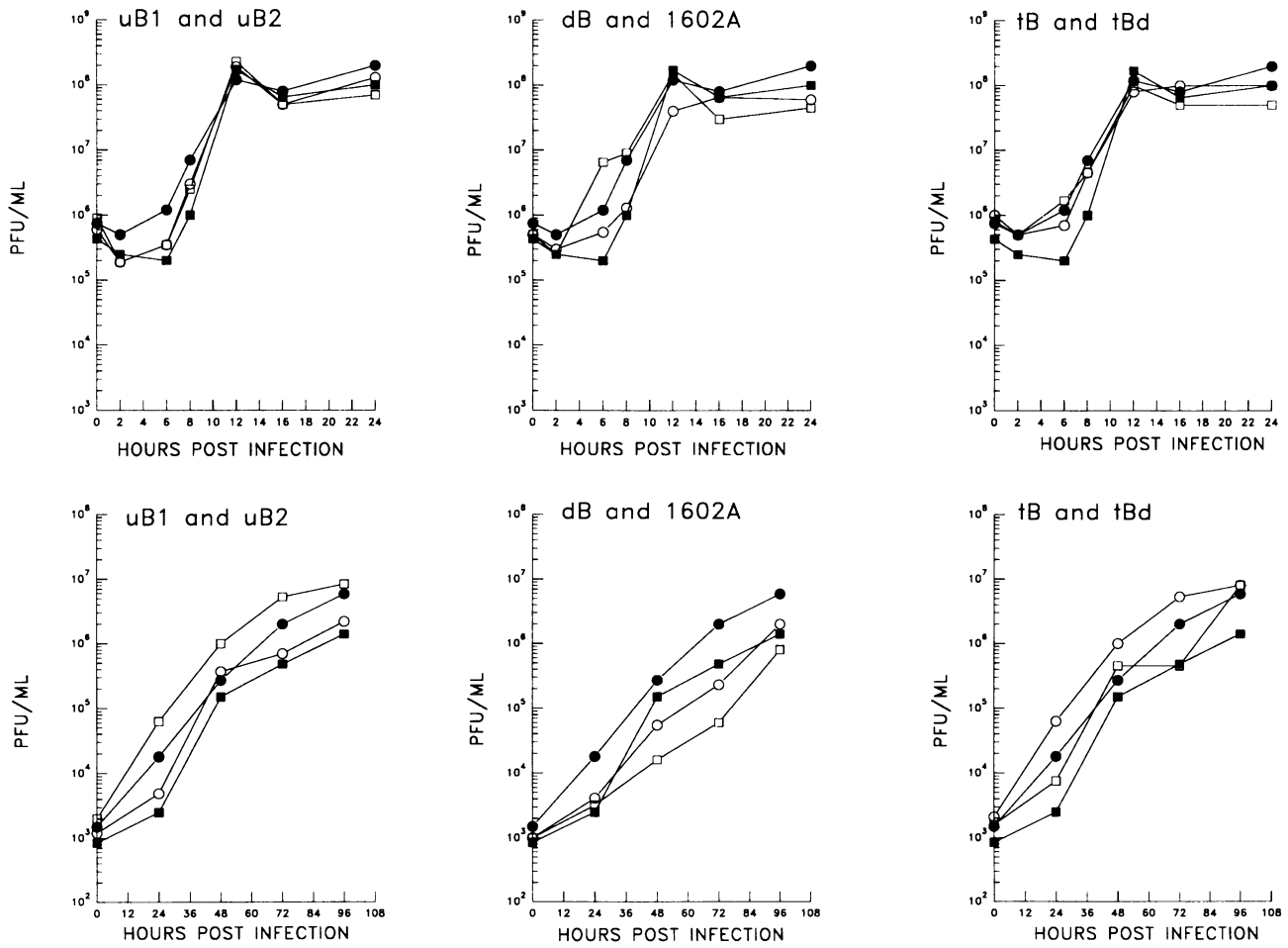

FIG. 3. Replication kinetic analyses with NIH 3T3 cells. Triplicate cultures of NIH 3T3 cells were infected at an MOI of 3 to 5 (top panels) or 0.01 (lower panels) PFU per cell. At the indicated times postinfection, the stocks were harvested and subjected to three cycles of freezing and thawing, and then the viral titers were determined on RSC monolayers. The results are plotted against the 3B1 and 3B2 data on each graph. For each virus, the titer of the inoculum is indicated as the zero-time point. Symbols: ●, 3B1; ■, 3B2; ○, uB1, tB, and dB; □, uB2, tBd, and 1602A.

rim) due to the loss of β-gal activity but immunohistochemically stained red (gray cells within the plaque) following in situ hybridization with the DIG-labeled β-gal probe. For each virus, at least 30% of the previously mapped mutant plaques were tested for the presence of β-gal sequences. All of the plaques tested contained β-gal sequences by this assay and therefore could not be attributed to contaminating wild-type virus. These data confirmed that the RMFs established for all of the viral mutants were accurate and not inflated because of contaminating wild-type virus.

RMF of HSV-1 following passage in murine cells. The data compiled from RMF analysis of two independent passage stocks generated from low-MOI infections of NIH 3T3 cells (designated P1 and P1′) are summarized in Fig. 5. Statistical significance of the differences in the data was examined by using chi-square analysis with the Yates continuity factor to compare the RMF of each virus with the wild-type blue RMF established by analysis of 3B1 and 3B2. Differences resulting in P values of <0.05 were considered significant and are indicated.

To establish the baseline RMF of a 17syn$^+$ derivative in which the UNG, TK, and dUTPase genes were unaltered, the passage stocks of control viruses 3B1 and 3B2 were examined. These strains carried the β-gal insert at the UL3 locus (bp 10959 to 11664), which was chosen because it is dispensable for viral replication in cultured cells (1) and does not encode a known enzyme activity involved in DNA replication. Two independent viruses were isolated to limit the possibility that unselected, second-site mutations would alter the findings.

Analysis of the P1 and P1′ stocks of 3B1 and 3B2 demonstrated the HSV-1 baseline RMF in NIH 3T3 cells to be between 0.4 and 0.6% or one mutant in 178 to 243 PFU (Fig. 5). This finding is consistent with the range of frequencies reported for HSV-1 strains (18–20, 31, 40, 41). Chi-square analysis demonstrated no statistically significant difference between 3B1 and 3B2 for either the P1 or P1′ passage. Comparison of P1 and P1′ stock RMFs demonstrated the reproducibility of the assay, with estimated P values of 0.54 and 0.37 for 3B1 P1 versus P1′ and 3B2 P1 versus P1′, respectively.

Although no selective advantage or disadvantage of β-gal activity was observed in the replication kinetic analysis (Fig. 3), it was possible that mutant plaque frequency could be affected by successive replication. To control for such a possibility, a high-MOI passage (HP) stock was generated from NIH 3T3 cells following infection with 3 to 5 PFU per cell. No significant difference was found between the RMFs of 3B1 and 3B2 P1,

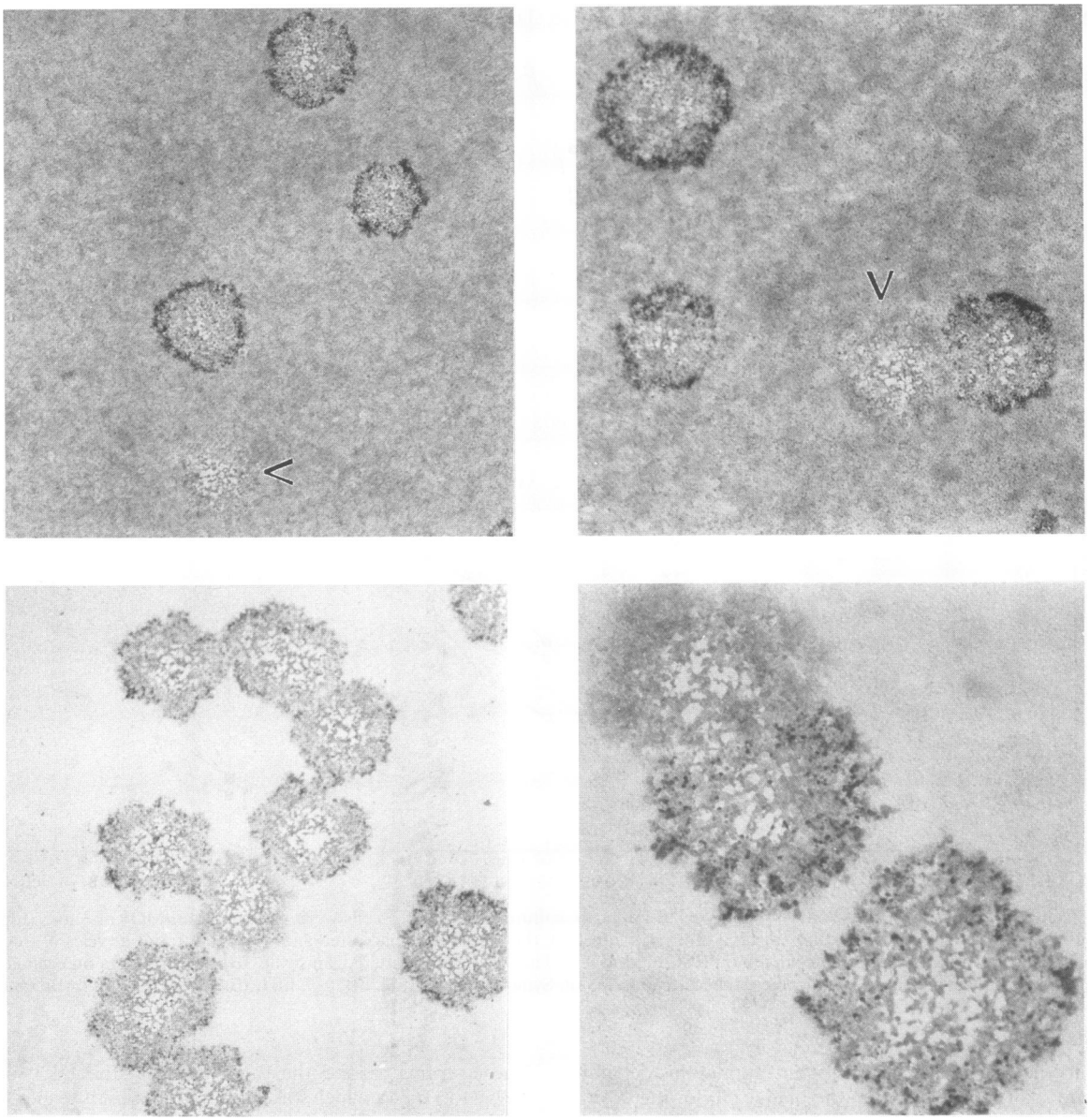

FIG. 4. Photomicrographs of the RMF plaque assay. Analysis of the passage stocks was completed by plating of ~2,000 PFU/100-mm-diameter RSC monolayer. Plaques were maintained in medium containing anti-HSV serum and then, at 48 h postinfection, fixed and stained with X-Gal. β-Gal activity resulted in a blue precipitate, as seen in the top two panels (cells with β-gal activity appear dark and are located at the plaque rim). Plaques which did not produce β-gal activity (mutants indicated by arrowheads) also became visible in the top two panels after counterstaining with Ponceau S. To confirm that the clear plaques were true mutants and not wild-type contaminants, in situ hybridization with a DIG-labeled, β-gal-specific probe was performed. Following immunolocalization of the DIG, positive in situ hybridization resulted in staining of the plaque center (labeled cells appear gray at the center of the plaque). The bottom two panels represent true mutants that contained the β-gal gene but lacked β-gal activity.

P1′, or HP stocks. However, a marginally significant difference ($P = 0.047$) was demonstrated when the 3B1 and 3B2 HP stocks were compared. The results of the HP stocks are presented graphically in Fig. 6. A second passage (P2) of the P1 stock also was completed by infecting NIH 3T3 cells at 0.01 PFU per cell. The data from the P2 stocks (Fig. 6) were consistent with the RMFs established for the P1, P1′, and HP stocks.

The contribution of the HSV-1 UNG, dUTPase, and TK activities to the viral RMF. UNG activity removes potentially mutagenic uracil residues from DNA that are present because of misincorporation by DNA *pol* or spontaneous cytosine deaminations (27). If cytosine deaminations are not repaired, a C-to-T transition is expected to occur, suggesting a direct role for UNG in determining the viral RMF. The data compiled from examination of the P1 and P1′ passage stocks of uB1 and uB2 demonstrated that the HSV-1 UNG activity does not appreciably affect the RMF following limited passage in NIH 3T3 cells. The RMFs established for both uB1 and uB2 were equivalent to the baseline RMF (0.4 to 0.5% or one mutant in 188 to 267 PFU; Fig. 5). Consistent with the observation that the MOI had no significant effect on the RMF of 3B1 or 3B2,

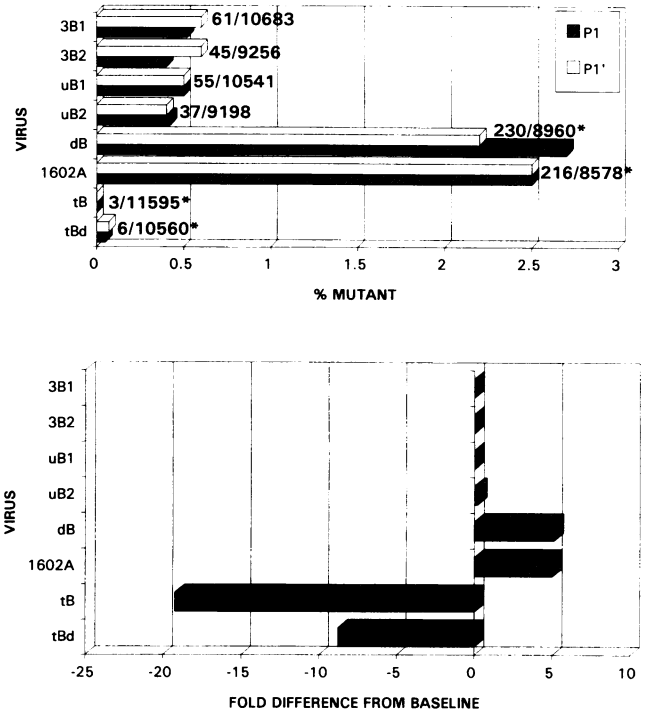

FIG. 5. Estimated RMF of P1 and P1′ viral stocks generated in NIH 3T3 cells. The results of the mutant plaque assay applied to two independently generated low-MOI (0.01 PFU per cell) passage stocks (P1 and P1′) are presented. The statistical significance of the differences in the data was analyzed by chi-square analysis with the Yates continuity factor. Each of the RMFs was compared with the RMFs of the control 3B1 and 3B2 virus stocks. The RMFs that were found to be significantly different from those of the controls ($P < 0.05$) are indicated with asterisks. The results are presented as the percentages of the populations that were found to be mutants. The fraction next to each bar represents the total plaque count with the number of mutants observed divided by the total number of plaques. The lower graph demonstrates the fold difference from the baseline RMF (0.5%) for each of the virus stocks.

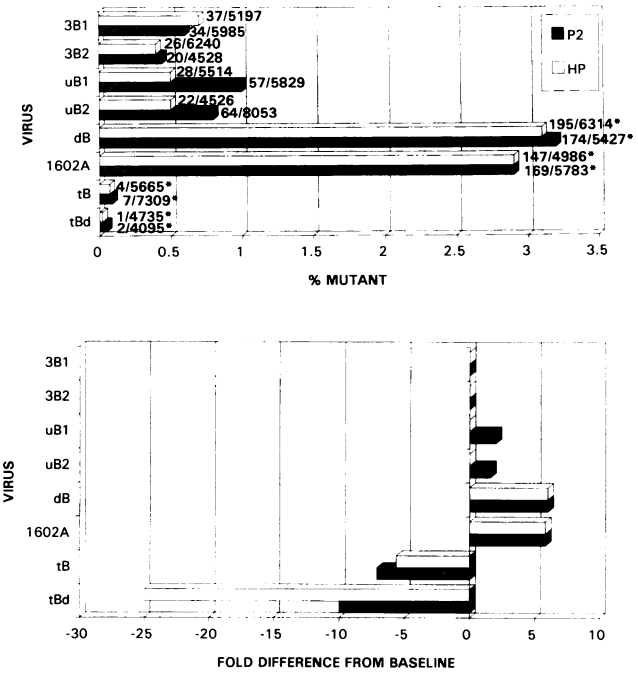

FIG. 6. Estimated RMF of P2 and HP viral stocks generated in NIH 3T3 cells. As described in the text, a P2 stock was generated by low-MOI (0.01 PFU per cell) infection of NIH 3T3 cells with the P1 stocks of each virus. The original virus stocks were also used to generate an HP stock following high-MOI (3 to 5 PFU per cell) infection of NIH 3T3 cells. The results of the RMF assays of these viral stocks are presented as described in the legend to Fig. 5.

no difference was observed between the RMFs of the HP stock and the low-MOI stocks of uB1 or uB2 (Fig. 5 and 6). Successive passages of uB1 and uB2 (P2 in Fig. 6) resulted in stocks with RMFs that were significantly increased (twofold; Fig. 6, lower graph) compared with the uB1 and uB2 RMFs observed in the P1 and P1′ passages (P1 stocks versus the P2 stock, $P = 0.001$).

It was of interest to determine if the viral dUTPase activity, which should also reduce dUTP misincorporation, would contribute to the RMF. A significant increase in the frequency of clear plaques from the baseline RMF was observed in the P1 and P1′ stocks of dUTPase-negative viruses dB and 1602A (2.5 and 2%, respectively; Fig. 5). This finding clearly established that the HSV-1-encoded dUTPase provides an antimutator function. In these stocks, a mutant plaque occurred as frequently as 1 in 40, significantly more often than in 3B1 or 3B2 ($P < 0.00001$). These results are not attributed easily to unselected, secondary mutations since dB and 1602A were derived from different parental viruses (17syn$^+$ and dUTPase-negative 17syn$^+$ mutant dUT$^-$1218, respectively) and carry the β-gal gene at different loci (Fig. 1).

The P2 stock of dB demonstrated a significant increase in RMF from the RMF established in the P1 stocks ($P = 0.03$; Fig. 6). This RMF was the highest observed in any of the NIH 3T3 virus passage stocks. The 1602A P2 stock also had a slight but not significant increase in the RMF compared with the P1 stocks ($P = 0.17$). The RMFs in the HP stocks of dB and 1602A were not significantly different from those of the low-MOI passage stocks (Fig. 5 and 6).

HSV TK activity primarily converts thymidine to TMP but also phosphorylates deoxycytidine and nucleoside analogs that are the basis for some successful antiherpes therapies. Examination of the TK$^-$ virus passage stocks clearly demonstrated a mutator function associated with this enzyme activity. The P1 and P1′ stocks of the two mutants which lack TK, tB and tBd, were found to contain a minimal number of mutant plaques (Fig. 5). The P1 RMFs were found to be 5- to 20-fold less than the baseline (Fig. 5, lower graph). Having established an appreciable RMF increase associated with loss of dUTPase activity in both dB and 1602A, we found that the mutator activity of TK was even more dramatic, since a 50-fold difference in RMF was observed between tBd (TK and dUTPase negative) and 1602A (UNG and dUTPase negative) in the P1 stocks. The RMFs established for the tB and tBd P2 and HP stocks were consistent with the RMFs of the P1 stocks (Fig. 5 and 6).

Viral RMFs following passage in LM TK$^-$ cells. To determine if the observed RMFs were affected significantly by the cellular environment provided by NIH 3T3 cells, a low-MOI passage of selected viruses was performed with LM TK$^-$ cells. LM TK$^-$ cells were chosen to determine if the loss of a cellular enzyme activity involved in nucleotide pool size regulation would measurably affect the viral RMF. The results of the RMF analysis of the passage stocks are presented in Fig. 7.

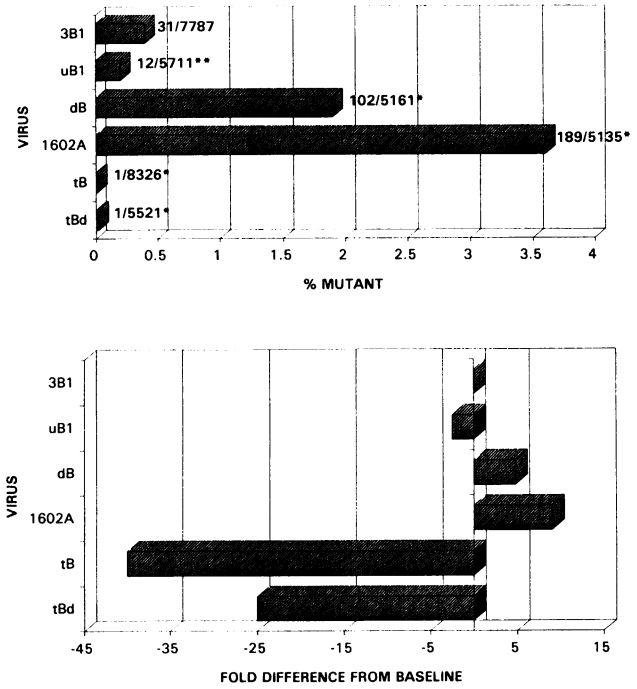

FIG. 7. Estimated RMFs of viral stocks generated in LM TK$^-$ cells. A low-MOI (0.01 PFU per cell) infection of LM TK$^-$ cells was performed with the indicated viruses, as described in the text. The RMFs of the resulting stocks were assayed, and the results are presented graphically as indicated in the legend to Fig. 5. Significant differences from the LM TK$^-$ 3B1 stock are denoted with single asterisks. Significant differences between the RMF established in the P1 stock generated in NIH 3T3 cells and the RMF in the LM TK$^-$ cell-generated viral stock are indicated with double asterisks.

The RMF of the 3B1 stock generated from LM TK$^-$ cell infection was the lowest of the RMFs observed for this virus (Fig. 5, 6, and 7); however, the difference from the RMF established in the NIH 3T3 P1 stocks was not significant (P1 stocks versus LM TK$^-$ P1 stock, $P = 0.12$). These results confirm an averaged baseline RMF for 17syn$^+$ derivatives of ~0.5%. Analysis of the uB1 passage stock generated in LM TK$^-$ cells demonstrated a significant decrease in the number of mutant plaques (Fig. 5 versus Fig. 7; P1 stocks versus LM TK$^-$ P1 stock, $P = 0.005$). This reduction was consistent with a slight antimutator effect for UNG activity and suggests that the NIH 3T3 cellular environment was better able to compensate the UNG mutation.

Both the dB and 1602A LM TK$^-$ cell passages had RMFs that demonstrated that the antimutator function associated with dUTPase activity was not specific to NIH 3T3 cells. The LM TK$^-$ dB stock RMF was significantly lower than the RMF observed in the dB NIH 3T3 P1 stock ($P = 0.033$) but was still fivefold greater than that of the LM TK$^-$ 3B1 stock (Fig. 7). This finding was consistent with the general trend of reduced RMF in the LM TK$^-$ cell environment. In contrast, the 1602A LM TK$^-$ stock had a significantly increased RMF compared with the NIH 3T3 P1 stocks (P1 stocks versus LM TK$^-$ P1 stock, $P = 0.0002$; Fig. 5 versus Fig. 7), suggesting that the LM TK$^-$ cellular environment was less able to compensate the mutations present in 1602A. In the 1602A LM TK$^-$ stock, a mutant was observed approximately every 27 plaques (3.8%; Fig. 7). Despite the lack of cellular TK, both the tB and tBd stocks showed RMFs equivalent to those established in NIH 3T3 cells (Fig. 7).

DISCUSSION

The evidence presented in this report demonstrates that the HSV-1-encoded TK and dUTPase significantly contribute to viral RMFs following viral propagation in two murine cell lines. In addition, a role for the HSV-1 UNG in determining the viral RMF was suggested by the serial passage of two independent UNG$^-$ viral stocks. The baseline viral RMF of 0.5% was established in stocks of two independent 17syn$^+$ UL3–β-gal strains that encode unaltered UNG, TK, and dUTPase activities (Fig. 5, 6, and 7). It should be noted that the function of the HSV-1 UL3 gene product has not been established; therefore, it is possible that this gene product plays a role in controlling the viral RMF. However, the baseline RMF established with these two viruses is consistent with the RMFs reported for other wild-type HSV-1 strains (18–20, 31, 40, 41). The reproducibility of this assay is evident by comparison of two independent passages following low-MOI infection (P1 and P1′ in Fig. 5). Passage of 3B1 in the LM TK$^-$ cell line also demonstrated that the established baseline RMF was not specific to the NIH 3T3 cellular environment (Fig. 7).

The HSV-1 strains examined in this study that lacked a functional TK activity had the highest-fidelity replication of any of the viruses examined. The tB passage stocks demonstrated the fewest mutants of any of the passage stocks and had RMFs that were up to 40-fold reduced from the baseline. Analysis of double mutant tBd, which lacked both TK and dUTPase activities, demonstrated the significance of the mutator function associated with TK activity, since viruses lacking dUTPase activity had RMFs up to fivefold greater than the baseline. It is possible that the RMFs observed for tB and tBd were due to a compensatory mutation. It is unlikely that this is the case, however, because tB was derived directly from 17syn$^+$ while tBd was generated from 17syn$^+$-derived, dUTPase-negative strain dUT$^-$1218. It is more likely, therefore, that the reduced RMFs are due to the loss of TK activity.

A possible explanation for the increased RMF associated with a functional HSV-1 TK may be found in the broad range of substrates recognized by this enzyme (reviewed in reference 16). In addition to phosphorylating nucleotides which are useful for DNA replication, the TK activity phosphorylates nucleoside analogs which can lead to termination of DNA synthesis (6–8). The nucleotide-binding site in the TK protein has been indicated (16), suggesting that TK activities with limited substrate specificity could be engineered and then assayed in this system. In fact, drug-resistant HSV-1 strains encoding TK proteins with reduced substrate specificity already have been reported (26, 47). Analysis of these altered TK genes in a strain with a known baseline RMF should help elucidate the mechanism by which TK contributes to the RMF.

The explanation for the antimutator function associated with the viral dUTPase is less obvious. As noted above, the stocks of dUTPase-negative virus dB had RMFs fivefold higher than the background. Consistent with these findings, dUTPase activity has been shown to serve an antimutator function in other systems (34, 37). The activity of dUTPase results in the reduction of dUTP pools and indirectly increases available dTTP pools (9, 24, 25). On the basis of the reduced RMF which results from loss of TK activity, reductions in the dTTP pool do not easily explain the altered RMF. Conversion of the dUTP pool to dUMP may reduce RMFs, but misincorporation of dUTP would be expected to be repaired by the cellular or viral UNG activity in the cell during infection (11, 27). If uracil

residues are not removed, a mutation does not necessarily occur; however, the presence of uracil residues in DNA may affect the proper functioning of regulatory sequences (15, 48). It is therefore unlikely that either of these possibilities fully explains the contribution of dUTPase. Identification of the regions of the HSV-1 dUTPase which are important for enzyme activity and viral characteristics is in progress and may help to elucidate the contribution of this enzyme to the viral RMF.

UNG activity was expected to increase the fidelity of DNA replication by removal of uracil because of misincorporation and from spontaneous deamination of cytosine residues in DNA (27). Such deaminations are potentially mutagenic, as they result in a G:C-to-A:T transition if not repaired, and may be of great concern following extended periods of HSV-1 latency in a host (30). In other systems, UNG activity has been demonstrated to be more effective on the G:U mismatch resulting from deaminations (49) and important for reduction of mutation frequencies (21, 34, 37). In support of a similar antimutator function for the HSV-1 UNG, successive passages of uB1 and uB2 resulted in a significant increase in the RMF (Fig. 6, P2) compared with both the P1 and P2 stocks of 3B1 and 3B2. It is attractive to hypothesize that in a UNG^- background with time or successive passage, the number of cytosine deaminations would build up, leading to an increase in the RMF. Analysis of successive passages (P3, P4, etc.) may lend support to this theory. It also would be interesting to establish the RMF of virus recovered from reactivations following increasing periods of latency; however, preliminary studies have been impeded by the minimal amounts of virus recovered.

dUTPase-negative, UNG^- double mutant 1602A was expected to have an increased RMF because of an increased probability of dUTP misincorporation and a reduced ability to remove such bases. Consistent with these predictions, the 1602A passage stocks had some of the highest RMFs of any of the stocks examined. It is possible that the NIH 3T3 cellular environment is able to compensate partially for the viral UNG mutation, since passage in LM TK^- cells resulted in a 1602A stock with the highest RMF observed (one mutant in 27 PFU; Fig. 7).

The RMF assay reported here provides a more versatile system for assessment of the contribution of virally encoded factors, for several reasons. The results obtained with this system are based upon loss of β-gal activity, which should not have affected viral replication, providing no selective advantage or disadvantage. Previous studies assayed for mutations of the TK gene (18–20, 31, 40, 41), which, although dispensable for viral replication in cultured cells, has been shown in this work to contribute dramatically to the viral RMF. The RMF assay in prior studies selected for a drug resistance phenotype to quantitate altered progeny, which may have limited the scoring of mutations. The RMF differences could be due, in part, to the use of different wild-type HSV-1 strains in the different studies as well as the cell lines used to generate the passage stocks. In this study, all of the viruses examined were derived originally from the HSV-1 $17syn^+$ strain and were passaged in two murine cell lines to demonstrate clearly the contribution of the virally encoded UNG, TK, and dUTPase to the viral RMF.

A possible limitation of this assay is the effect of the context of the β-gal gene in the viral genome. Specific regions of the genome may be more or less prone to mutation, leading in this assay to greater or fewer clear plaques. However, dUTPase-negative viruses dB and 1602A, which carry β-gal insertions at opposite ends of the unique long region (Fig. 1), demonstrated no difference between their RMFs, suggesting that the context has a limited effect or these two regions of the genome have similar mutation potentials.

The reported RMFs in this study were not artificially inflated because of contamination of the passage stocks with wild-type, β-gal gene-negative virus, since in situ hybridization demonstrated that 100% of the mutant plaques tested contained β-gal sequences. The MOI also can be eliminated as a possible concern, since RMFs of stocks generated by infection with 0.01 PFU per cell (Fig. 5) were consistent with the RMFs observed following high-MOI passage (3 to 5 PFU per cell; Fig. 6). The RMFs of the 3B1 and 3B2 HP stocks were not significantly different from the P1 RMFs (Fig. 5 and 6), also suggesting that there was no selection for or against viruses which lacked a functional β-gal gene.

HSV-encoded TK, dUTPase, and UNG activities are dispensable for efficient viral replication (14, 23, 30); however, all three enzymes have been shown to play important roles in viral replication in vivo (13, 32, 33). Although no replication deficiency of dUTPase-negative or UNG^- viral strains has been observed in vitro, it is likely that these enzymes promote increased fidelity of DNA synthesis. Having established that HSV-1 encodes several genes which affect the viral RMF in addition to the viral DNA *pol* (20), antiviral therapies which inhibit the function of mutator activities or enhance the activity of antimutators may increase the effectiveness of present therapies.

ACKNOWLEDGMENTS

This research was supported by Public Health Service grants NS 25879 from the National Institute of Neurological and Communicative Disorders and Stroke and AI 22667 and AI 32121 from the National Institute of Allergy and Infectious Diseases to L. Stanberry and R.L.T. R.B.P. was the recipient of an Albert J. Ryan Foundation predoctoral fellowship.

The advice and viruses provided by D. McGeoch were greatly appreciated.

REFERENCES

1. **Baines, J. D., and B. Roizman.** 1991. The open reading frames U_L3, U_L4, U_L10, and U_L16 are dispensable for the replication of herpes simplex virus 1 in cell culture. J. Virol. **65**:938–944.
2. **Bernstein, C., H. Bernstein, S. Mufti, and B. Strom.** 1972. Stimulation of mutation in phage T4 by lesions in gene 32 and by thymidine imbalance. Mutat. Res. **16**:113–119.
3. **Burns, W. H., et al.** 1982. Isolation and characterisation of resistant herpes simplex virus after acyclovir therapy. Lancet **i**:421–423.
4. **Challberg, M. D., and T. J. Kelly.** 1989. Animal virus DNA replication. Annu. Rev. Biochem. **58**:671–717.
5. **Coen, C. M., and P. A. Schaffer.** 1980. Two distinct loci confer resistance to acycloguanosine on herpes simplex virus type 1. Proc. Natl. Acad. Sci. USA **77**:2265–2269.
6. **Coen, D. M.** 1990. Antiviral drug resistance. Ann. N. Y. Acad. Sci. **616**:224–237.
7. **Coen, D. M.** 1991. The implications of resistance to antiviral agents for herpesvirus drug targets and therapy. Antiviral Res. **15**:287–300.
8. **Crumpacker, C. S.** 1989. Molecular targets of antiviral therapy. N. Engl. J. Med. **321**:163–172.
9. **Daikoku, T., N. Yamamoto, K. Maeno, and Y. Nishiyama.** 1991. Role of viral ribonucleotide reductase in the increase of dTTP pool size in herpes simplex virus-infected Vero cells. J. Gen. Virol. **72**:1441–1444.
10. **Drake, J. W.** 1969. Genetic control of mutation rates in bacteriophage T4. Nature (London) **221**:1128–1132.
11. **Duker, N., and C. L. Grant.** 1980. Alterations in the levels of deoxyuridine triphosphatase, uracil-DNA glycosylase and AP endonuclease during the cell cycle. Exp. Cell Res. **125**:493–497.

12. **Erlich, K. S., J. Mills, P. Chatis, G. J. Mertz, D. F. Busch, S. E. Follansbee, R. M. Grant, and C. S. Crumpacker.** 1989. Acyclovir-resistant herpes simplex virus infections in patients with the acquired immunodeficiency syndrome. N. Engl. J. Med. **320:**293–296.
13. **Field, H. J., and P. Wildy.** 1978. The pathogenicity of thymidine kinase-deficient mutants of herpes simplex virus in mice. J. Hyg. **81:**267–277.
14. **Fisher, F. B., and V. G. Preston.** 1986. Isolation and characterization of HSV-1 mutants which fail to induce dUTPase activity. Virology **148:**190–197.
15. **Focher, F., A. Verri, S. Verzeletti, P. Mazzarello, and S. Spadari.** 1992. Uracil in OriS of herpes simplex virus 1 alters its specific recognition by origin binding protein (OBP): does virus induced uracil-DNA glycosylase play a key role in viral reactivation and replication? Chromosoma **102:**S67–S71.
16. **Gentry, G. A.** 1992. Viral thymidine kinases and their relatives. Pharmacol. Ther. **54:**319–355.
17. **Glorioso, J., W. F. Goins, and D. J. Fink.** 1992. Herpes simplex virus-based vectors. Semin. Virol. **3:**265–276.
18. **Hall, J. D., and R. E. Almy.** 1982. Evidence for the control of herpes simplex virus mutagenesis by the viral DNA polymerase. Virology **116:**535–543.
19. **Hall, J. D., D. M. Coen, B. L. Fisher, M. Weisslitz, S. Randall, R. E. Almy, P. T. Gelep, and P. A. Schaffer.** 1984. Generation of diversity in herpes simplex virus: an antimutator phenotype maps to the DNA polymerase locus. Virology **132:**26–37.
20. **Hall, J. D., P. A. Furman, M. H. St. Clair, and C. W. Knopf.** 1985. Reduced in vivo mutagenesis by mutant herpes simplex DNA polymerase involves improved nucleotide selection. Proc. Natl. Acad. Sci. USA **82:**3889–3893.
21. **Holliday, R.** 1985. Aspects of DNA repair and nucleotide pool imbalance, p. 453–460. *In* F. J. de Serres (ed.), Genetic consequences of nucleotide pool imbalance. Plenum Press, New York.
22. **Jamieson, A. T., G. A. Gentry, and J. H. Subak-Sharpe.** 1974. Induction of both thymidine and deoxycytidine kinase activity by herpes viruses. J. Gen. Virol. **24:**465–480.
23. **Kit, S., and D. R. Dubbs.** 1965. Properties of deoxythymidine kinase partially purified from noninfected and virus-infected mouse fibroblast cells. Virology **26:**16–27.
24. **Kornberg, A.** 1980. DNA replication, p. 52–64. W. H. Freeman & Co., San Francisco.
25. **Kunz, B. A., and S. E. Kohalmi.** 1991. Modulation of mutagenesis by deoxynucleotide levels. Annu. Rev. Genet. **25:**339–359.
26. **Larder, B. A., Y. Cheng, and G. Darby.** 1983. Characterization of abnormal thymidine kinases induced by drug-resistant strains of herpes simplex virus type 1. J. Gen. Virol. **64:**523–532.
27. **Lindahl, T.** 1979. DNA glycosylases, endonucleases for apurinic/apyrimidinic sites, and base excision repair. Prog. Nucleic Acid Res. **22:**135–192.
28. **Lo, K., and M. J. Bessman.** 1976. An antimutator deoxyribonucleic acid polymerase. J. Biol. Chem. **251:**2480–2486.
29. **McGeoch, D. J., M. A. Dalrymple, A. J. Davison, A. Dolan, M. C. Frame, D. McNab, L. J. Perry, J. E. Scott, and P. Taylor.** 1988. The complete sequence of the long unique region in the genome of herpes simplex virus type 1. J. Gen. Virol. **69:**1531–1574.
30. **Mullaney, J., H. W. Moss, and D. J. McGeoch.** 1989. Gene UL2 of herpes simplex virus type 1 encodes a uracil-DNA glycosylase. J. Gen. Virol. **70:**449–454.
31. **Parris, D. S., and J. E. Harrington.** 1982. Herpes simplex virus variants resistant to high concentrations of acyclovir exist in clinical isolates. Antimicrob. Agents Chemother. **22:**71–77.
31a. **Pyles, R. B., et al.** Unpublished data.
32. **Pyles, R. B., N. M. Sawtell, and R. L. Thompson.** 1992. Herpes simplex virus type 1 dUTPase mutants are attenuated for neurovirulence, neuroinvasiveness, and reactivation from latency. J. Virol. **66:**6706–6713.
33. **Pyles, R. B., and R. L. Thompson.** Evidence that the herpes simplex virus type 1 uracil DNA glycosylase is required for efficient viral replication and latency in the murine nervous system. J. Virol., in press.
34. **Richards, R. G., O. Brown, and W. D. Sedwick.** 1985. Misincorporation of deoxyuridine in human cells: consequences of antifolate exposure, p. 149–162. *In* F. J. de Serres (ed.), Genetic consequences of nucleotide pool imbalance. Plenum Press, New York.
35. **Roizman, B., and A. E. Sears.** 1990. Herpes simplex viruses and their replication, p. 1795–1841. *In* B. N. Fields et al. (ed.), Virology, 2nd ed. Raven Press, New York.
36. **Schnipper, L. L., and C. S. Crumpacker.** 1980. Resistance of herpes simplex virus to acycloguanosine: role of viral thymidine kinase and DNA polymerase loci. Proc. Natl. Acad. Sci. USA **77:**2270–2273.
37. **Sedwick, W. D., O. E. Brown, and B. W. Glickman.** 1986. Deoxyuridine misincorporation causes site-specific mutational lesions in the *lacI* gene of *Escherichia coli*. Mutat. Res. **162:**7–20.
38. **Sibrack, C. D., C. McLaren, and D. W. Barry.** 1982. Disease and latency characteristics of clinical herpes simplex isolates after acyclovir therapy. Am. J. Med. **37:**372–375.
39. **Smith, G. H.** 1987. In situ detection of transcription in transfected cells using biotin-labeled molecular probes. Methods Enzymol. **151:**530–539.
40. **Smith, K. O.** 1963. Some biological aspects of herpesvirus-cell interactions in the presence of 5-iodo, 2-desoxyuridine (IDU). J. Immunol. **91:**582–590.
41. **Smith, K. O., W. L. Kennell, R. H. Poirier, and F. T. Lynd.** 1980. In vitro and in vivo resistance of herpes simplex virus to 9-(2-hydroxyethoxymethyl)guanine (acycloguanosine). Antimicrob. Agents Chemother. **17:**144–150.
42. **Sonkin, P. L., K. H. Baratz, R. Frothingham, and L. M. Cobo.** 1992. Acyclovir resistant herpes simplex virus keratouveitis after penetrating keratoplasty. Ophthalmology **99:**1805–1808.
43. **Southern, E. M.** 1975. Detection of specific sequences among DNA fragments separated by gel electrophoresis. J. Mol. Biol. **98:**503–517.
44. **Speyer, J. F.** 1965. Mutagenic DNA polymerase. Biochem. Biophys. Res. Commun. **21:**6–8.
45. **Tenser, R. B.** 1991. Role of herpes simplex virus thymidine kinase expression in viral pathogenesis and latency. Intervirology **32:**76–92.
46. **Thompson, R. L., E. K. Wagner, and J. G. Stevens.** 1983. Physical location of a herpes simplex virus type-1 gene function(s) specifically associated with a 10 million-fold increase in HSV neurovirulence. Virology **131:**180–192.
47. **Veerisetty, V., and G. A. Gentry.** 1983. Alterations in substrate specificity and physicochemical properties of deoxythymidine kinase of a drug-resistant herpes simplex virus type 1 mutant. J. Virol. **46:**901–908.
48. **Verri, A., P. Mazzarello, G. Biamonti, S. Spadari, and F. Focher.** 1990. The specific binding of nuclear proteins to the cAMP responsive element (CRE) sequence (TGACGTCA) is reduced by the misincorporation of U and increased by the deamination of C. Nucleic Acids Res. **18:**5775–5780.
49. **Verri, A., P. Mazzarello, S. Spadari, and F. Focher.** 1992. Uracil-DNA glycosylases preferentially excise mispaired uracil. Biochem. J. **287:**1007–1010.
50. **Williams, M. V.** 1988. Herpes simplex virus-induced dUTPase: target site for antiviral chemotherapy. Virology **166:**262–264.